CrystEngComm

RSC Publishing

PAPER

View Article Online
View Journal

Characterization of Bridgman grown GaSe:Al crystals

Cite this: DOI: 10.1039/c3ce40116b

J. Guo,[a] J.-J. Xie,[a] L.-M. Zhang,[a] D.-J. Li,[a] G.-L. Yang,[a] Yu. M. Andreev,[bc] K. A. Kokh,*[d] G. V. Lanskii,[bc] A. V. Shabalina,[c] A. V. Shaiduko[bc] and V. A. Svetlichnyi[c]

Downloaded by Washington University in St. Louis on 11/04/2013 10:17:36.
Published on 28 February 2013 on http://pubs.rsc.org | doi:10.1039/C3CE40116B

Received 20th January 2013,
Accepted 27th February 2013

DOI: 10.1039/c3ce40116b

www.rsc.org/crystengcomm

Centimeter-sized Al-doped nonlinear GaSe crystals were grown by the modified Bridgman method with heat field rotation. The alumina distribution coefficient in the grown crystals was estimated to be about 8 $\times$ 10^{-2} for GaSe:Al ($\geqslant$0.1 at%) crystals. GaSe:Al ($\leqslant$0.5 at%) crystals possess optical properties suitable for non-linear applications. For the first time the increase in the ordinary refractive index of GaSe crystals with doping was demonstrated to be different to other doped GaSe crystals.

Introduction

Widely used ε-GaSe nonlinear crystals are characterized by very weak mechanical properties. On the other hand, the existence of III–VI compounds with structures similar to that of GaSe (GaS, GaTe, InSe) suggest deep doping with sulfur (S), tellurium (Te) and indium (In) by the growth of solid solutions.[1,2] It was proved by many researchers that incorporation of different doping elements at high content noticeably modifies the physical properties responsible for frequency conversion efficiency in GaSe. Allakhverdiev *et al.*[3] had shown that sulfur doping of GaSe results in a decrease in the nonlinearity coefficient d_{22}, but variation of S-content in the crystal allows one to control the mid-IR dispersions. For the first time ~84% improvement in the efficient non-linearity in GaSe by In doping was reported by Suhre *et al.*[4] and later confirmed in ref. 5. Frequency conversion into the THz range was demonstrated in Te-doped GaSe[6] and was maximized by the optimal content of the dopant in ref. 7. It was ascertained in all studies that the increase in the efficiency is caused by the improvement in the crystal optical quality. Even in spite of the nonlinearity decreasing,[3] it was established that the set of modified physical properties of S-doped GaSe has resulted in 2.4 times higher CO_2 laser SHG efficiency compared to that in pure GaSe crystal.[8] Besides, it was demonstrated that o-wave dispersion in the THz range decreases with S[9–11] and Te[7] doping that can be used for phase matching control.

One more interesting doping approach concerns the introduction of non-isomorphous atoms into the GaSe structure. Chen *et al.*[12] have reported the doping by 0.5 at% of heavy (atomic weight is 126 g mol^{-1}) Er in GaSe that resulted in a 24% increase in intrinsic non-linearity up to a magnitude of 55.3 pm V^{-1}. The increased non-linearity was attributed to the substitutive and interstitial doping of Er ions into the GaSe unit cell. The ErSe compound exists[13] but there is no data on the layered ErSe structure or the possibility to form solid solution crystals with GaSe.

Another promising doping agent is Al.[14] Although it is able to form some similar compounds with Ga (for instance GaN–AlN), no information about the existence of AlSe was found. Al_2Se and $AlSe_2$ compounds are stable only at a vapor phase but Al_2Se_3 and Ga_2Se_3 form different defected structures: wurtzite and zincblende, respectively.[15] However, it was ascertained that optical quality GaSe:Al crystals can be grown by the conventional Bridgman technique from the melt with low, $\leqslant$0.05 wt% (0.14 at%), Al content in the charge composition.[14] From these data Al-doped GaSe crystals possesses minimal, down to $\leqslant 10^{-7}$ ohm^{-1} cm^{-1}, conductivity along the (001) surface among doped GaSe crystals, as well as increased mobility and decreased life time of free charge carriers. It should be emphasized that improved hardness up to 17 kg mm^{-2} has allowed cutting and polishing the crystal at arbitrary directions. No changes of optical properties (mid-IR transparency, dispersions and phase matching conditions) compared with pure GaSe were found for these crystals except a small shift of the short-wave transmission end towards long waves. Taking into account the strong change of electrophysical properties of GaSe:Al[14] and relative effect on dielectric response it can be proposed that noticeable changes should occur in the optical properties of Al-doped GaSe in the THz range.

In this work we report characterization of GaSe crystals grown by the modified Bridgman technique from the melts containing 0.01, 0.05, 0.1, 0.2, 0.5, 1, 2 at% of Al.

[a]*Key Laboratory of Laser Interaction with Matter, Changchun Institute of Optics, Fine Mechanics and Physics, CAS, 3888 Dongnanhu Road, Changchun, 130033, China. E-mail: lightcoming@163.com; Fax: +86-431-846-682-31; Tel: +86-135-043-269-17*
[b]*Laboratory of Geosphere–Biosphere Interactions, Institute of Monitoring of Climatic and Ecological Systems SB RAS, 10/3 Akademichesky Av., Tomsk, 634055, Russia. E-mail: yuandreev@yandex.ru; Fax: +7 3822-491-950; Tel: +7 960-971-1540*
[c]*Laboratory of Advanced Materials and Technologies, Siberian Physical–Technical Institute of Tomsk State University, 1 Novosobornaya Sq., Tomsk, 634050, Russia. E-mail: v_svetlichnyi@bk.ru; Fax: +7 3822-533-034; Tel: +7 903-954-6245*
[d]*Laboratory of Crystal Growth, Institute of Geology and Mineralogy, SB RAS, Novosibirsk 90, 630090, Russia. E-mail: k.a.kokh@gmail.com; Fax: +7 383 33066392; Tel: +7 383 33066392*

This journal is © The Royal Society of Chemistry 2013

Published on 28 February 2013 on http://pubs.rsc.org | doi:10.1039/C3CE40116B
Downloaded by Washington University in St. Louis on 11/04/2013 10:17:36.

Crystal growth and characterization methods

The starting materials for the synthesis were Ga 99.9997, S 99.99 and Al 99.95. Synthesis of stoichiometric GaSe was performed according to the steps described in detail in ref. 16. The synthesized polycrystalline material was then reloaded to the growth ampoules with required addition of elementary Al. The dimensions of the ampoule for growth were 150 mm in length, including 30 mm conical tip, and 10 mm diameter. All the ampoules were evacuated to a residual pressure $\sim 10^{-4}$ Torr. After charging, the sealed off ampoules were heated up to 1000 °C and kept for several days in order to dissolve the dopant. The last step was a slow unseeded crystallization by the modified Bridgman technique with a heat field rotation. Each ampoule was mechanically pulled down at a speed 5 mm day^{-1} through the temperature gradient $\sim$15 K cm^{-1} at the level of the crystallization front. Details on the design of the modified Bridgman furnace may be found in ref. 17. The optical properties of pure GaSe and available GaSe:S (1 wt% or 2.285 at%) crystals, described elsewhere,[7,8,18] were studied in the THz range for comparison. The samples were cleaved along the (001) layers from as-grown ingots; no additional treatment or polishing of surfaces was made. Hall measurement system used in ref. 14 was exploited to measure conductivity of the GaSe:Al crystals.

Optical quality and external view of grown GaSe:Al crystals are demonstrated in Fig. 1.

Structural properties of grown crystals were observed by transmission electron microscopy (TEM) with a scanning microscope CM12 (Philips). The nonlinear method[19] was applied to identify polytypes. Electron probe micro analyses (EPMA) method with a JXA-8800M (JEOL) device were used for measurement of Ga and Se contents. The atomic emission spectrometry method with inductively-coupled plasma optical emission spectrometry (ICP-OES) was used to measure the Al content. An ICP-OE spectrometer iCAP 6500 (Thermo Scientific) with a detection limit about 10^{-4} and standard deviation 0.05–0.15 was exploited in this case.

UV-visible transparency spectra were recorded by a Cary 100 Scan (Varian Inc.) spectrophotometer: wavelength range 190–900 nm, spectral resolution $\Delta\lambda$ = 0.2–4 nm, wavelength deviation $\pm$1 nm. Mid-IR optical spectra were recorded by a FTIR Nicolet 6700 spectrometer. The operation wavelength range is 11 000–375 cm^{-1}, spectral resolution is 0.09 cm^{-1}.

The optical properties of grown crystals were measured by the standard terahertz (THz) time-domain spectroscopy method (THz-TDS)[20] in the range of 0.4–2.5 THz. The THz pulses were generated by a home-made biased 5 × 5 × 1 mm InP photoconductive switch under the pumping of Ti:Sapphire laser pulses (λ = 790 nm, τ = 80 fs).[21] Transmitted THz pulses were detected by free-space electro-optic sampling method by means of a 1 mm-thick (110) ZnTe crystal. In this study, the THz beam was normally incident to the crystal surface.

Raman spectra were recorded by a Raman-Fourier spectrometer Nicolet NXR 9650 (Thermo Electron Corp.): $\Delta\lambda$ = 3500–100 cm^{-1}, spectral resolution 0.8 cm^{-1} pumped with a Nd:YAG laser at 1.064 μm.

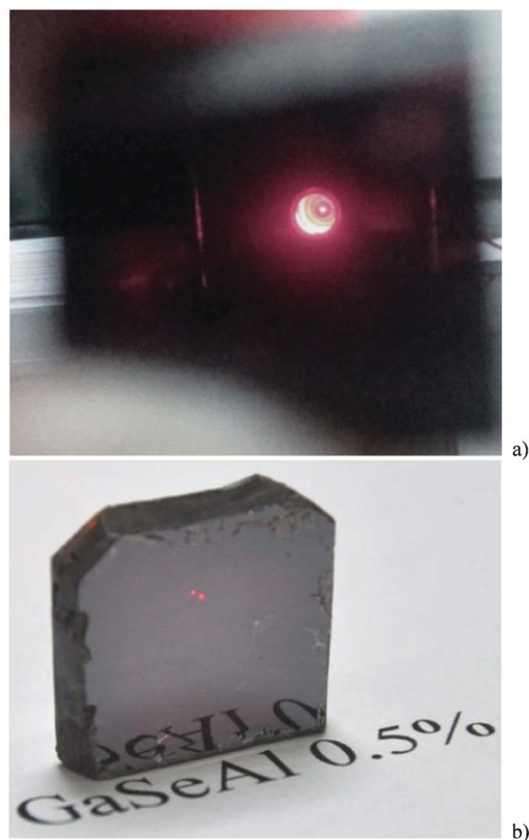

Fig. 1 (a) View on the output mirror of operating He–Ne laser through 10 mm GaSe:Al (0.2 at%) crystal and (b) cleaved GaSe:Al (0.5 at%) crystal exposed to semiconductor 0.655 μm laser beam.

Results and discussion

Visual control of the Al-doped crystals has shown that due to the geometrical selection phenomenon all ingots became single crystalline approximately $\sim$30–40 mm from the tip. The samples cleaved from nose to central sections of the GaSe:Al ($\leqslant$0.5 at%) ingots appeared to be of optical quality and suitable for nonlinear applications (Fig. 1). A small segregation was observed in the end section of the GaSe:Al (0.5 at%) ingot. The GaSe:Al (1 at%) ingot was polycrystalline because of inclusions, but the small samples were suitable for studying optical properties, while the GaSe:Al (2 at%) ingot was useless because of precipitation. Therefore, a very low solubility of Al in GaSe may be suggested.

Chemical analysis has shown that Ga and Se contents are well within the homogeneity range;[22] selenium content was about 1 at% lower than Ga content. Al content in the grown ingots was significantly lower to that in the melt compositions. We were unavailable to measure the reliable Al content in the crystal grown from the melt with 0.01 at% of Al. The averaged

 This journal is © The Royal Society of Chemistry 2013

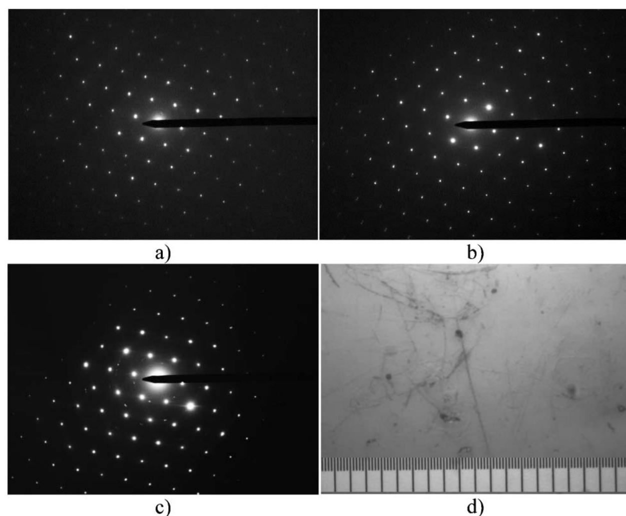

Fig. 2 SAED patterns observed by TEM for (a) GaSe, (b) GaSe:Al (0.2 at%), and (c) GaSe:Al (0.5 at%) and (d) surface micro defects in GaSe:Al (1 at%). Electron beam is directed along [001]. Minimal scale division is 10 μm.

Published on 28 February 2013 on http://pubs.rsc.org | doi:10.1039/C3CE40116B
Downloaded by Washington University in St. Louis on 11/04/2013 10:17:36.

concentration for selected sections of each ingot grown from the melts with 0.05 to 0.5 at% of Al was taken into account, while analyses with higher Al content were considered as a result of the interference of Al-rich precipitations or surface micro defects. According to our data, in the selected optical quality GaSe: (0.5 ⩾ Al ⩾ 0.1 at%) crystals the Al distribution coefficient were estimated to be about 8×10^{-2}. So, solubility of Al in GaSe is low and hard to measure by EPMA.[14] Moreover, the EPMA reflexes of Al and Se are strongly overlapped. Due to the difficulties in reliable composition measurement we will label the grown crystals in accordance with the melt composition for the given crystals.

By means of the TEM it was observed that Al-doped crystals possess similar hexagonal structures to pure GaSe (Fig. 2). However the structure defects undoubtedly appear at the doping level of 0.5 at% Al (Fig. 2c). It was found that the SAED patterns at this and higher doping levels were varying point to point due to the presence of disordered linear and local point micro defects and precipitations (Fig. 2d). φ-Angle dependence of the output signal for CO_2 laser I type second harmonic generation in GaSe:Al (⩽0.5 at%) crystals was a six-petal-flower type similar to that for pure ε-GaSe in full accordance with the nonlinear method of GaSe structure characterization.[19] These results confirm the availability of GaSe:Al (⩽0.5 at%) for nonlinear applications. Application of heavily doped crystals was limited by the Al-containing precipitations. However, very thin films of GaSe:Al (1 at%) were still suitable for local points THz generation under fs Ti:Sapphire laser pump.

Electrophysic data have shown that the conductivity of pure GaSe is about 4×10^{-2} ohm^{-1} cm^{-1} and gradually decreases with alumina content, reaching $\sim 10^{-7}$ ohm^{-1} cm^{-1} in GaSe:Al (0.5 at%). Measurement data show a four orders of magnitude decrease of charge carrier (holes) concentration from the initial value of $\geqslant 10^{16}$ cm^{-3}. It is known that hole-type conductivity in GaSe is due to Ga vacancies.[1] And from first principle estimations it has been shown that substitution of Ga vacancies is the most probable process in the initial stage of ref. 23. Therefore it may be proposed that the decrease in the concentration of free charge carriers is the result of substitution of Ga vacancies by chemically similar Al atoms. It should be noted that Ga atoms form $(Ga–Ga)^{4+}$ dimer units in the structure of GaSe.[24] Thus, the mechanism of Al introduction is not clear, *i.e.* it embeds as a part of the dimer (formal oxidation state of two) or as a separate cation (Al^{+3}).

No evident shift in the short- and long-wave transmission ends was found for a 50 μm thick sample from crystals grown by modified technology in contrast to data reported in ref. 14. It can be proposed that both low solubility and close atomic weight of Al and Ga atoms does not lead to a significant change in the primitive cell weight and basic optical properties of GaSe crystal. Nevertheless, a small monotonic increase in the intensity of the exciton absorption peak and simultaneously in the phonon absorption band at 450 cm^{-1} was observable with the increase in the Al content. The phonon absorption band at 450 cm^{-1} is attributed to the localized mode due to the presence of uncontrolled impurities in pure GaSe.[25] Rising up of the intensity of this short-wavelength phonon band confirms the incorporation of light Al atoms into the GaSe lattice. We were unable to measure reliably the changes in the optical extinction coefficient in the mid-IR transmission window in the GaSe:Al (⩽0.2 at%) crystals due to small absorptivity but increased absorption was easily measured for 5 mm and longer GaSe:Al (⩾0.5 at%) crystals. These absorption coefficients were from two to three times lower to that reported in ref. 14 for close composition crystals grown by the conventional technology.

Study of Raman spectra has shown small changes in scattering patterns that confirm Al incorporation into GaSe. In particular, a monotonic change was observed with Al-doping in the intensity distribution between two Raman bands at about 209 cm^{-1} (it is due to rigid layer phonon mode E'') and 213 cm^{-1} (it is due to rigid layer phonon mode E'(TO))[25] (Fig. 3).

Significant changes in the optical properties of GaSe:Al crystals have been observed by THz-TDS in the THz range in sub-mm to 2 mm long samples. Selected o-wave absorption spectra measured by THz-TDS are depicted in Fig. 4. The optical quality of the GaSe crystal at the short-wave (⩾1.5 THz) THz range became improved at low, 0.05 at% of Al doping. The absorption coefficient has insignificantly risen up for the GaSe:Al (0.5 at%) crystal and noticeably rises up with further doping similar to that in the mid-IR. However, this increase in the absorption coefficient is not so fatal for THz applications of Al-doped GaSe crystals due to exploitation of thin, μm-scale length, samples. The absorption coefficient in pure GaSe ranges from 2 cm^{-1} to 7 cm^{-1},[26,27] while it is below 12 cm^{-1} in the selected points of GaSe:Al (⩽1 at%) crystals.

To estimate the complex dielectric function for the ordinary polarized wave in the THz range for fabricated z-cut crystals, it

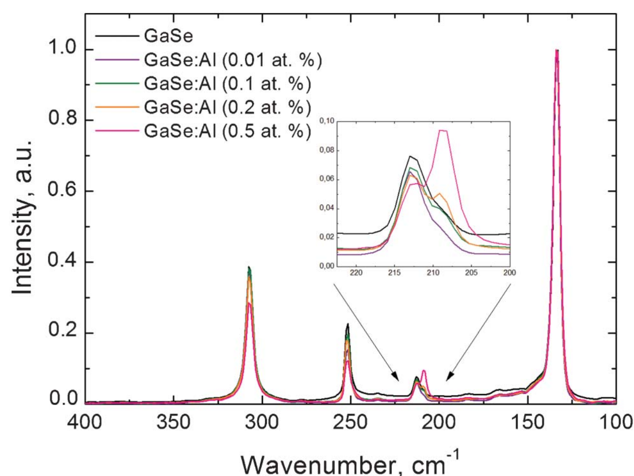

Fig. 3 Raman spectra for pure and Al-doped GaSe crystals.

is necessary to consider inputs of the transverse lattice vibration (phonon) and free carriers (electrons or plasma). In accordance with the combined Drude–Lorentz model, the total dielectric function (ω)[28] for an orthogonal incident wave in this case is given by

$$\tilde{\varepsilon}(\omega)=\varepsilon(\infty)+\sum_{j-1}^{J}\frac{S_j\omega_{TOj}^2}{\omega_{TOj}^2-\omega^2-i\Gamma_j\omega}-\frac{\omega_p^2}{\omega\left(\omega+i\langle\tau\rangle^{-1}\right)} \quad (1)$$

where S_j is the strength of the oscillator, $\omega_{\mathrm{TO}j}$ is the frequency of the transverse optical phonon, Γ_j the phonon relaxation rate, ω_{p} is the plasma frequency, and $\langle\tau\rangle$ is the average momentum relaxation time for the free electron. The first term of the right-hand side, $\varepsilon(\infty)$, is the high-frequency dielectric constant related to bound electrons; the second term describes the contribution of optical phonons; and the third term is the contribution from plasma. Ordinary wave dispersion can be written as $n(\omega) = \mathrm{Re}[\varepsilon(\omega)]^{1/2}$. By relating to eqn (1) it appears that the $n(\omega)$ response in doped GaSe crystals depends on the relative position of transverse optical phonons and plasma frequency, phonons and average momentum relaxation times, strength of phonon oscillators and plasma frequency, that depends on free electron density. In accordance with ref. 20 (page 21) plasma frequency ω_{p} can be estimated by

$$\omega_p=\sqrt{\frac{Nq^2}{m\varepsilon_0}} \quad (2)$$

where N is the density of free electrons; q and m are electron charge and efficient mass, respectively; ε_0 is the permittivity of light in free space.

The frequency $\omega_{E'(\mathrm{TO})}$ of the most intensive fundamental transverse phonon mode $E'(\mathrm{TO})$ in GaSe is centered at 6.42 THz (213 cm^{-1}).[29] Typically, for semiconducting materials $N_{\mathrm{p}} \approx 10^{16}$ cm^{-3}, as well as for selected samples of pure GaSe in this study, and that is why ω_{p} is > 6 THz.[20] So, a very intensive fundamental phonon mode $E'(\mathrm{TO})$ and plasma are likely to be the dominant factors that determine the same sign of the dielectric response in pure GaSe at the nearby short-wavelength part of the THz range. In principle, the small input of other known long-wave phonon modes that are of much lower intensity and centered at: $A_1' - A_2''(\mathrm{LO})$ at 1.84 THz (61.3 cm^{-1}), $A_1' - E'(\mathrm{LO})$ at 1.57 THz (52.3 cm^{-1}), $E'(\mathrm{LO}) - E''$ at 1.24 THz (41.3 cm^{-1}), $A_2''(\mathrm{TO}) - E''$ at 0.8 THz (26.6 cm^{-1}),[28] $E'^{(2)}$ at 0.59 THz (19.88 cm^{-1})[29] also have to be accounted for.

S and Te doping in GaSe crystal decreases free carrier density within 10 to $\leqslant$30 times.[30] As a result, plasma frequency ω_{p} should be shifted from fundamental phonon mode frequency $\omega_{E'(\mathrm{TO})}$ into short-wave part of THz range. Additional influence in the dielectric response can be predicted from a few more processes: changes in the lattice parameters, changes in the rigid layer phonon mode $E'^{(2)}(\mathrm{TO})$ at 0.59 THz (Fig. 4) that disappear with heavy doping, and also by simultaneous rising up of the rigid layer mode $E''^{(2)}(\mathrm{TO})$ at ~1.78 THz.[7] In addition, changes in the probability of interactions (live time or $\langle\tau\rangle$) of free charge carriers with doping has also to be accounted for. Thus, the relative input of the plasma in the dielectric response of S and Te-doped crystals has complicated dependence on the dopant concentration, the spectral gap between $\omega_{E'(\mathrm{TO})}$ and ω_{p} and the other above mentioned factors. Consequently, a decrease in the ordinary refractive index was observed in GaSe with S[10–12] and Te[7,11] doping.

On the other hand, Al-doping in GaSe results in more than four orders of magnitude lower conductivity that makes the relationship $\omega_{\mathrm{p}} \ll \omega_{E'(\mathrm{TO})}$ undoubtedly valid. In this case the input of the most intensive and low intensity phonon modes in the dielectric response can be neglected and it will be governed by the following equation[28]

$$\varepsilon(\omega)=\varepsilon_\infty-\frac{\omega_p^2}{\omega\left(\omega+i\langle\tau\rangle^{-1}\right)} \quad (3)$$

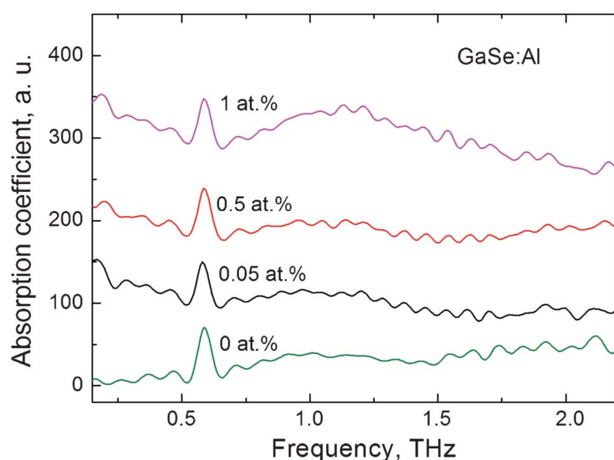

Fig. 4 Spectra of o-wave dispersion in pure and doped GaSe:Al crystals.

Downloaded by Washington University in St. Louis on 11/04/2013 10:17:36.
Published on 28 February 2013 on http://pubs.rsc.org | doi:10.1039/C3CE40116B

 This journal is © The Royal Society of Chemistry 2013

Downloaded by Washington University in St. Louis on 11/04/2013 10:17:36.
Published on 28 February 2013 on http://pubs.rsc.org | doi:10.1039/C3CE40116B

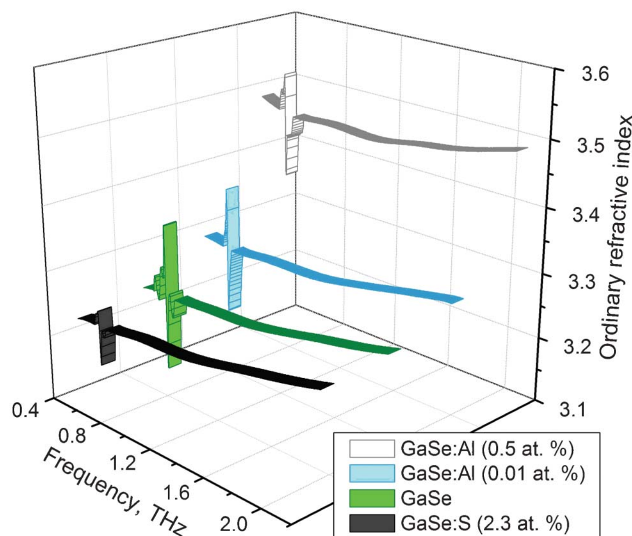

Fig. 5 -Wave refractive index dispersion in pure and doped GaSe crystals.

Eqn (3) can be further approximated to

$$\varepsilon(\omega) = \varepsilon_\infty - \frac{\omega_p^2}{\omega^2} \quad (4)$$

because collisions between free electrons at low density are negligible and they can be considered to be moving freely.[20]

In accordance with eqn (4), the dielectric response of Al-doped crystal in the THz range has to increase with the decrease of free charge carrier density that also comes from the measurement results (Fig. 5).

Conclusions

Doped GaSe crystals were grown from the melts with 0.01, 0.05, 0.1, 0.2, 0.5, 1, 2 at% of Al by the modified Bridgman technology. The Al distribution coefficient was estimated to be about 8×10^{-2}. The optical quality of GaSe:Al ($\leqslant$0.5 at%) crystals is suitable for nonlinear applications in the mid-IR and THz range frequency converters. For the first time the increase in the ordinary refractive index of GaSe:Al was demonstrated.

Acknowledgements

This work is supported in part by RFBR, Projects No. 12-08-00482-a and 12-02-33174; Presidium SB RAS, MIP No.46 of 2012 and VIII.80.2.3; Presidential program SP-742/2012/1.

Notes and references

1 A. Gouskov, J. Camassel and L. Gouskov, *Prog. Cryst. Growth Charact.*, 1982, **5**, 323.
2 V. V. Atuchin, N. F. Beisel, K. A. Kokh, V. N. Kruchinin, I. V. Korolkov, L. D. Pokrovsky, A. R. Tsygankova and A. E. Kokh, *CrystEngComm*, 2013, **15**, 1365.
3 K. R. Allakhverdiev, R. I. Guliev, E. Yu. Salaev and V. V. Smirnov, *Sae Mulli*, 1982, **7**, 947.
4 D. R. Suhre, N. B. Singh, V. Balakrishna, N. C. Fernelius and F. K. Hopkins, *Opt. Lett.*, 1997, **22**, 775.
5 Z.-S. Feng, Z.-H. Kang, F.-G. Wu, J.-Yu. Gao, Yu. Jiang, H.-Z. Zhang, Yu. M. Andreev, G. V. Lanskii, V. V. Atuchin and T. A. Gavrilova, *Opt. Express*, 2008, **13**, 9978.
6 K. C. Mandal, S. H. Kang, M. Choi, J. Chen, X.-C. Zhang, J. M. Schleicher, C. A. Schmuttenmaer and N. C. Fernelius, *IEEE J. Sel. Top. Quantum Electron.*, 2008, **2**, 284.
7 S.-A. Ku, W.-C. Chu, C.-W. Luo, Y. M. Andreev, G. Lanskii, A. Shaiduko, T. Izaak, V. Svetlichnyi, K. H. Wu and T. Kobayashi, *Opt. Express*, 2012, **5**, 5029.
8 H.-Z. Zhang, Z.-H. Kang, Yu. Jiang, J.-Yu. Gao, F.-G. Wu, Z.-S. Feng, Yu. M. Andreev, G. V. Lanskii, A. N. Morozov, E. I. Sachkova and S. Yu. Sarkisov, *Opt. Express*, 2008, **13**, 9951.
9 Z.-W. Luo, X.-A. Gu, W.-C. Zhu, W.-C. Tang, Yu. Andreev, G. Lanskii, A. Morozov and V. Zuev, *Opt. Precis. Eng.*, 2011, **2**, 354.
10 L.-M. Zhang, J. Guo, D.-J. Li, J.-J. Xie, Yu. M. Andreev, V. A. Gorobets, V. V. Zuev, K. A. Kokh, G. V. Lanskii, V. O. Petukhov, V. A. Svetlichnyi and A. V. Shaiduko, *J. Appl. Spectrosc.*, 2011, **6**, 850.
11 S.-A. Ku, C.-W. Luo, Yu. M. Andreev and G. Lanskii, *Appl. Phys. Lett.*, 2012, **100**, 136103Comment on [*Appl. Phys. Lett.*, 2011, **99**, 081105].
12 Ch. W. Chen, Yu. K. Hsu, J. Y. Huang, Ch. Sh. Chang, J. Yu. Zhang and C. L. Pan, *Opt. Express*, 2006, **14**, 10636.
13 J. F. Miller, F. J. Reid and R. C. Himes, *J. Electrochem. Soc.*, 1959, **12**, 1043.
14 Y.-F. Zhang, R. Wang, Z.-H. Kang, L.-L. Qu, Y. Jiang, J.-Y. Gao, Yu. M. Andreev, G. V. Lanskii, K. A. Kokh, A. N. Morozov, A. V. Shaiduko and V. V. Zuev, *Opt. Commun.*, 2011, **284**, 1677.
15 C.-Y. Lu, J. A. Adams, Q. m. Yu, T. Ohta, M. A. Olmstead and F. S. Ohuchi, *Phys. Rev. B: Condens. Matter Mater. Phys.*, 2008, **78**, 075321.
16 K. A. Kokh, Yu. M. Andreev, V. A. Svetlichnyi, G. V. Lanskii and A. E. Kokh, *Cryst. Res. Technol.*, 2011, **46**, 327.
17 K. A. Kokh, B. G. Nenashev, A. E. Kokh and G. Yu. Shvedenkov, *J. Cryst. Growth*, 2005, **1–2**, E2129.
18 Z.-S. Feng, Z.-H. Kang, F.-G. Wu, J.-Yu. Gao, Yu. Jiang, H.-Z. Zhang, Yu. M. Andreev, G. V. Lanskii, V. V. Atuchin and T. A. Gavrilova, *Opt. Express*, 2008, **13**, 9978.
19 Yu. M. Andreev, K. A. Kokh, G. V. Lanskii and A. N. Morozov, *J. Cryst. Growth*, 2011, **1**, 1164.
20 Y.-S. Lee, *Principle of Terahertz Science and Technology*, Springer, New York, 2008, 340pp.
21 M. M. Nazarov, A. P. Shkurinov, A. A. Angeluts and D. A. Sapozhnikov, *Radiophys. Quantum Electron.*, 2009, **8**, 536.
22 V. I. Shtanov, A. A. Komov, M. E. Tamm, D. V. Atrashenko and V. P. Zlomanov, *Dokl. Chem.*, 1998, **1–3**, 140.
23 Zs. Rak, S. D. Mahanti, K. C. Mandal and N. C. Fernelius, *Phys. Rev. B: Condens. Matter Mater. Phys.*, 2010, **82**, 155203.
24 N. N. Greenwood and A. Earnshaw, *Chemistry of the Elements, Butterworth Heinemann*, Oxford, 2nd edn, 1987, 1345pp.

25 K. Allakhverdiev, T. Baykara, S. Ellialtioglu, F. Hashimzade, D. Huseinova, K. Kawamura, A. A. Kaya, A. M. Kulibekov and S. Onari, *Mater. Res. Bull.*, 2006, **41**, 751.
26 M. M. Nazarov and A. P. Shkurinov, *Izv. Vuzov. Radiofizika*, 2009, **7–8**, 1.
27 S.-A. Ku, W.-C. Chu, C.-W. Luo, A. A. Angeluts, M. G. Evdokimov, M. M. Nazarov, A. P. Shkurinov, Yu. M. Andreev, G. V. Lanskii, A. V. Shaiduko, K. A. Kokh and V. A. Svetlichnyi, *Chin. J. Opt.*, 2012, **1**, 57.
28 L. Yu, F. Zeng, V. Kartazayev, R. R. Alfano and K. C. Mandal, *Appl. Phys. Lett.*, 2005, **87**, 182104.
29 C.-W. Chen, Yu.-K. Hsu, J. Y. Huang and C.-S. Chang, *Opt. Express*, 2006, **22**, 10636.
30 A. A. Tikhomirov, Yu. M. Andreev, G. V. Lanskii, O. V. Voevodina and S. Yu. Sarkisov, *Proc. SPIE*, 2006, **6258**, 64.

Downloaded by Washington University in St. Louis on 11/04/2013 10:17:36.
Published on 28 February 2013 on http://pubs.rsc.org | doi:10.1039/C3CE40116B

 This journal is © The Royal Society of Chemistry 2013